RADC-TR-89-142
In-House Report
October 1989

DERIVATION AND APPLICATION OF DUAL-SURFACE INTEGRAL EQUATIONS FOR THREE-DIMENSIONAL, MULTI-WAVELENGTH PERFECT CONDUCTORS

Arthur D. Yaghjian and Margaret Woodworth

APPROVED FOR PUBLIC RELEASE; DISTRIBUTION UNLIMITED.

ROME AIR DEVELOPMENT CENTER
Air Force Systems Command
Griffiss Air Force Base, NY 13441-5700

This report has been reviewed by the RADC Public Affairs Office (PA) and is releasable to the National Technical Information Service (NTIS). At NTIS it will be releasable to the general public, including foreign nations.

RADC TR-89-142 has been reviewed and is approved for publication.

APPROVED:

J. LEON POIRIER
Chief, Applied Electromagnetics Division
Directorate of Electromagnetics

APPROVED:

JOHN K. SCHINDLER
Director of Electromagnetics

FOR THE COMMANDER:

JOHN A. RITZ
Directorate of Plans and Programs

If your address has changed or if you wish to be removed from the RADC mailing list, or if the addressee is no longer employed by your organization, please notify RADC (EECT) Hanscom AFB MA 01731-5000. This will assist us in maintaining a current mailing list.

Do not return copies of this report unless contractual obligations or notices on a specific document requires that it be returned.

REPORT DOCUMENTATION PAGE

Form Approved
OMB No. 0704-0188

1. AGENCY USE ONLY (Leave blank)	2. REPORT DATE	3. REPORT TYPE AND DATES COVERED
	October 1989	In-House Jan 88 to Dec 88

4. TITLE AND SUBTITLE
Derivation and Application of Dual-Surface Integral Equations for Three-Dimensional, Multi-wavelength Perfect Conductors

5. FUNDING NUMBERS
PE 61102F
PR 2305
TA J4
WU 10

6. AUTHOR(S)
Arthur D. Yaghjian and Margaret B. Woodworth

7. PERFORMING ORGANIZATION NAME(S) AND ADDRESS(ES)
Rome Air Development Center
RADC/EECT
Hanscom AFB
Massachusetts 01731-5000

8. PERFORMING ORGANIZATION REPORT NUMBER
RADC-TR-89-142

9. SPONSORING/MONITORING AGENCY NAME(S) AND ADDRESS(ES)

10. SPONSORING/MONITORING AGENCY REPORT NUMBER

11. SUPPLEMENTARY NOTES

12a. DISTRIBUTION/AVAILABILITY STATEMENT
Approved for public release, distribution unlimited

12b. DISTRIBUTION CODE

13. ABSTRACT (Maximum 200 words)
We derive the dual-surface electric- and magnetic-field integral equations for 3-D perfectly electrically conducting bodies, prove that they produce a unique solution at all real frequencies, and demonstrate their applicability to multi-wavelength bodies by solving the dual-surface magnetic-field integral equation for a rectangular scatterer using the method of conjugate gradients.

14. SUBJECT TERMS		15. NUMBER OF PAGES
Scattering Surface Integral Equations	Conjugate Gradient Method, [illegible]	40 16. PRICE CODE

17. SECURITY CLASSIFICATION OF REPORT	18. SECURITY CLASSIFICATION OF THIS PAGE	19. SECURITY CLASSIFICATION OF ABSTRACT	20. LIMITATION OF ABSTRACT
Unclassified	Unclassified	Unclassified	SAR

CONTENTS

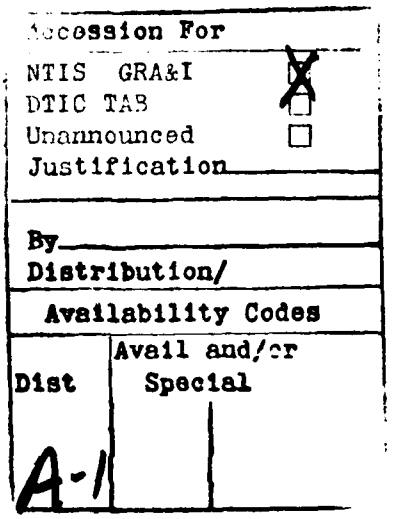

ILLUSTRATIONS

TABLES

DERIVATION AND APPLICATION OF DUAL-SURFACE INTEGRAL EQUATIONS FOR THREE-DIMENSIONAL, MULTI-WAVELENGTH PERFECT CONDUCTORS

1. INTRODUCTION

The numerical solution of dual-surface integral equations[1] applied to three-dimensional (3-D), multi-wavelength, perfectly conducting bodies can be obtained with readily available computers in a central processing unit (CPU) time proportional to approximately $(s/\lambda)^4 \ln (s/\lambda)$ using the conjugate gradient method[2] and direct access memory files[3] (s is the dimension of the body and λ the wavelength). Specifically, for a given incident field and aspect angle, the induced current and far field over 4π steradians of a perfectly conducting cube 5 wavelengths on a side is computed[4] in about

---

(Received for Publication 5 Oct 1989)

[1] Tobin, A.R., Yaghjian, A.D., and Bell, M.M. (1987) Surface integral equations for multi-wavelength, arbitrarily shaped, perfectly conducting bodies, *Digest of the National Radio Science Meeting (URSI)*, Boulder, CO, p. 9.

[2] Sarkar, T.K. and Arvas, E. (1985) On a class of finite step iterative methods (conjugate directions) for the solution of an operator equation arising in electromagnetics, *IEEE Trans. Antennas and Propagat.* AP-33: 1058-1066.

[3] Woodworth, M.B. (1988) *Large Matrix Solution Techniques Applied to an Electromagnetic Scattering Problem.* RADC-TR-88-268. ADA206917

[4] Cote, M.G., Woodworth, M.B., and Yaghjian, A.D. (1988) Scattering from the perfectly conducting cube, *IEEE Trans. Antennas Propagat.* AP-36: 1321-1329.

1.5 hours of CPU time [utilizing two-fold symmetry of the cube: see Eq. (34)] on a VAX 8650 computer with a "32-bit Linpack benchmark performance rating" of 1.3 megaflops.[5] The same computer would take about 11 hours of CPU time for this 5λ cube if the matrix of the dual-surface integral equation were solved using, instead of the conjugate gradient method, Gaussian elimination, which requires a computer time proportional to approximately $(s/\lambda)^6$. [Gaussian elimination CPU time with direct access files can be estimated from Eq. (30) with $N = 75(s/\lambda)^2$.] If the two-fold symmetry of the cube were not used to reduce the number of unknowns by a factor of 4 these CPU times using the conjugate gradient and Gaussian elimination methods would increase by factors of approximately 22 and 64, respectively, that is, from 1.5 and 11 hours to about 33 and 700 hours (30 days) of CPU time for a 5λ scatterer. This latter CPU time of 30 days confirms that scattering or radiation from arbitrarily shaped 5λ, 3-D bodies cannot be determined in a reasonable amount of computer time, using conventional Gaussian elimination, by a computer with a Linpack performance rating on the order of one megaflop. It becomes necessary to use faster matrix solution schemes, such as the conjugate gradient iterative method, when the integral equations are applied to progressively larger bodies, regardless of the speed of the computer.

Herein, we derive the dual-surface electric and magnetic-field integral equations for 3-D perfectly electrically conducting bodies, prove that they produce a unique solution at all real frequencies, and demonstrate their applicability to multi-wavelength bodies by solving the dual-surface magnetic-field integral equation for a rectangular scatterer using the method of conjugate gradients.

Magnetic-field surface integral equations for perfect conductors appeared in the literature as early as 1931[6], and both electric and magnetic-field surface integral equations were derived in Maue's definitive 1949 *Zeitschrift Fur Physik* paper.[7] However, only in the last ten years or so have digital computers become fast enough to solve these surface integral equations for arbitrarily shaped, 3-D, multi-wavelength bodies.

---

[5] Dongarra, J., Martin, J.L., and Worlton, J. (1987) Computer benchmarking: paths and pitfalls, *IEEE Spectrum*, 24: 38-43.

[6] Murray, F.H. (1931) Conductors in an electromagnetic field, *Am. J. Math.*, 53: 275-288.

[7] Maue, A.W. (1949) On the formulation of a general scattering problem by means of an integral equation, *Z. Phys.*, 126(7/9): 601-618.

Unfortunately, as Murray and Maue noted, the original electric and magnetic-field integral equations (EFIE and MFIE) fail to produce a unique exterior solution at frequencies equal to the resonant frequencies of the corresponding interior cavity. Since the density of cavity resonant frequencies increases rapidly beyond the first resonant frequency, which occurs when the dimension of a full-bodied 3-D scatterer equals about one wavelength, the numerical solution of 3-D, multi-wavelength bodies is severely hampered by these spurious resonances.

In Reference[8] it was proven that the original integral equations allow spurious solutions at the cavity resonant frequencies because at (and only at) these frequencies the MFIE does not restrict the tangential electric field to zero on the surface of the scatterer and the EFIE does not restrict the tangential magnetic field to $\bar{K} \times \hat{n}$ on the surface of the scatterer. ($\bar{K}$ is the surface current and $\hat{n}$ the outward unit normal to the scatterer. Interestingly, the MFIE result was also proven in the early paper by Murray.[6]) Among the alternatives that have been proposed for eliminating the spurious solutions from the original integral equations, the combined-field[9, 10, 11] or combined-source[12, 13, 14] integral equation, and the augmented electric or magnetic-field

---

[8] Yaghjian, A.D. (1981) Augmented electric and magnetic-field integral equations, *Radio Science*, **16**: 987-1001.

[9] Mitzner, K.M. (1968) Numerical solution of the exterior scattering problem at eigen-frequencies of the interior problem, *Digest of Fall URSI Meeting*, Boston, MA, p. 75.

[10] Poggio, A.J., and Miller, E.K. (1973) Integral equation solutions of three-dimensional scattering problems, in *Computer Techniques for Electromagnetics*, edited by R. Mittra, 159-264, Pergamon, New York.

[11] Mautz, J.R. and Harrington, R.F. (1978) H-field, E-field, and combined-field solutions for conducting bodies of revolution, *Arch. Elektron. Ubertragungstech. (Electron. Commun.)*, 32(4): 157-164.

[12] Panic, I.O. (1965) On the solvability of exterior boundary-value problems for the wave equation and for a system of Maxwell's equations, *Uspehi Mat. Nauk*, **20**(1): 221-226.

[13] Brakhage, H. and Werner, P. (1965) Uber das Dirichletsche Aussenraumproblem fur die Helmholtzsche Schwingungsgleichung, *Arch. Math.*, **16**: 325-329.

[14] Mautz, J.R. and Harrington, R.F. (1979) A combined-source solution for radiation and scattering from a perfectly conducting body, *IEEE Trans. Antennas and Propagation*, **AP-27**: 445-454.

integral equation[8] appear the more generally applicable and effective in numerical practice. However, for arbitrarily shaped, 3-D, multi-wavelength bodies, the combined and augmented integral equations also have their drawbacks. The combined-field and combined-source equations involve the operators of both the magnetic-field equation and the electric-field equation, which takes considerably more programming ingenuity and computer time than the original MFIE to achieve the same accuracy of solution. The augmented MFIE involves only the magnetic-field operator, but the augmented integral equations require a special procedure to eliminate all the spurious solutions from bodies of revolution.

Thus, we begin the integral equation solution for arbitrarily shaped, 3-D, multi-wavelength perfect conductors with the derivation of dual-surface electric and magnetic-field integral equations that differ only slightly from the original electric and magnetic-field integral equations, yet eliminate all spurious solutions. The dual-surface magnetic-field integral equation was given in Reference 1, but the derivation and proof of uniqueness of the dual-surface magnetic and electric-field integral equations have not appeared previously. Recently, Toyoda et al.[15] presented an "extended integral equation formulation" for 2-D scatterers that used additional surfaces near the surface of the scatterer. Their formulation for perfect conductors applies an extended integral equation to an interior surface and requires the interior surface to move with frequency to maintain uniqueness of solution. The derivation of the dual-surface magnetic and electric-field integral equations, (5a) and (5b), in the following section requires the introduction of a second surface interior and parallel to the surface of the scatterer, but the resulting integral equations have a unique solution at all real frequencies and are applied to the single surface of the scatterer.

2. DERIVATION OF DUAL-SURFACE INTEGRAL EQUATIONS

A time harmonic [exp ($-i\omega t$), ω real and > 0] electromagnetic field ($\bar{E}_{inc}$, $\bar{H}_{inc}$) incident in free space upon the surface S of a perfectly electrically conducting

---

[15] Toyoda, I., Matsuhara, M., and Kumagai, N. (1988) Extended integral equation formulation for scattering problems from a cylindrical scatterer, *IEEE Trans. Antennas and Propagat.* **36**: 1580-1586.

scatterer excites a surface current $\bar{K}$. (Let S be coincident with the surface current $\bar{K}$.) Since the total field inside the scatterer is zero, the scattered fields equal the negative of the incident fields inside S, and one can write the "interior" or "extended" integral equations,

$$-\bar{H}_{inc}(\bar{r}) = \int_S \bar{K}(\bar{r}') \times \nabla'\psi(\bar{r},\bar{r}')dS' \qquad (1a)$$

($\bar{r}$ inside S)

$$E_{inc}(\bar{r}) = \frac{1}{i\omega\varepsilon_o} \int_S \left[k^2 \bar{K}\psi - (\nabla'_S \cdot \bar{K})\nabla'\psi\right]dS', \qquad (1b)$$

where $k(=\omega/c=2\pi/\lambda)$ is the free-space propagation constant, ε_o is the permittivity of free space, and $\psi(\bar{r},\bar{r}')$ is the free-space Green's function $\exp(ik|\bar{r}-\bar{r}'|)/4\pi|\bar{r}-\bar{r}'|$.

Let the observation point $\bar{r}$ in Eqs. (1a) and (1b) approach the surface S of the conductor from inside S, and convert the surface integrations in Eq. (1) to circular principal-value integrations using the following formula (derived by a straightforward integration near the singularity of ψ[8]):

$$\int_{S(\bar{r},S)} \nabla'\psi \, dS' = \oint_S \nabla'\psi \, dS' - \frac{\hat{n}}{2}, \qquad (2)$$

where $\oint_S$ denotes the principal-value surface integration evaluated by excluding the singular point, $\bar{r}'=\bar{r}$, of the integrand by a limiting circular "principal area" centered on $\bar{r}$, and $\hat{n}$ is the outward unit normal from the surface S at $\bar{r}$. Eqs. (1) then yield the augmented magnetic and electric-field surface integral equations[8] for the exterior scattering problem:

$$-\bar{H}_{inc}(\bar{r}) = \frac{1}{2}\,\hat{n} \times \bar{K} + \oint_S \bar{K} \times \nabla'\psi \, dS' \qquad (3a)$$

$(\bar{r}$ on $S)$

$$E_{inc}(\bar{r}) = \frac{(\nabla_s \cdot \bar{K})\hat{n}}{2\,i\omega\varepsilon_o} + \frac{1}{i\omega\varepsilon_o} \oint_S \left[k^2\,\bar{K}\psi - (\nabla'_s \cdot \bar{K})\nabla'\psi\right] dS'. \qquad (3b)$$

Taking $\hat{n}$ cross these overdetermined Eqs. (3) reduces them to the original even determined MFIE and EFIE,

$$\hat{n} \times \bar{H}_{inc} = \frac{1}{2}\,\bar{K} - \hat{n} \times \oint_S \bar{K} \times \nabla'\psi \, dS' \qquad (4a)$$

$(\bar{r}$ on $S)$

$$\hat{n} \times \bar{E}_{inc} = \frac{\hat{n}}{i\omega\varepsilon_o} \times \oint_S \left[k^2\,\bar{K}\psi - (\nabla'_s \cdot \bar{K})\nabla'\psi\right] dS'. \qquad (4b)$$

As mentioned in the Introduction, the original integral Eqs. (4) are plagued by spurious solutions for $\bar{K}$ at the resonant frequencies of the cavity formed by the surface S. Although either of the augmented Eqs. (3) eliminate the spurious solutions for most shapes, they must both be used, in general, to eliminate all the spurious resonances when the surface S is a body of revolution. The combined-field integral equation[9, 10, 11] eliminates the spurious resonances by adding Eq. (4a) to $-\alpha_o \hat{n}$ crossed into Eq. (4b), and uniqueness of solution of the combined-source equation[12, 13, 14] follows from its operator being the adjoint of the combined-field operator[11, 14]. (The real constant α_o is often chosen equal to the free-space wave admittance.)

To derive the dual-surface integral equations, return to the extended integral equations (1). The current $\bar{K}(\bar{r})$ in Eq. (1a) or (1b) is uniquely determined at every

frequency if Eq. (1a) or (1b) is satisfied for all $\bar{r}$ inside S[16]. Conceivably, one could determine the current $\bar{K}$ by solving numerically the vastly overdetermined set of extended integral equations that results from Eq. (1a) or (1b) applied to points $\bar{r}$ separated by a small fraction of a wavelength throughout the volume enclosed by S. Or one could supplement the surface integral equations (4) with the extended integral equations (1) applied at selected points $\bar{r}$ within S.[17,18,19] The former approach introduces a prohibitive number of equations for multi-wavelength bodies, and in applying the latter approach one has no convenient, reliable criterion for selecting the number and position of the interior points at which the extended integral equations (1a) and (1b)must be satisfied to assure Eqs. (4a) and (4b) produce the correct unique current $\bar{K}$ at all frequencies. (The modified Green's function method[20,21,22] for eliminating the spurious solutions from the original surface integral equations (4) suffers from a similar uncertainty in choosing the proper number and origin of eigenfunctions in the representation of the modified Green's function.[23])

---

[16] Waterman, P.C. (1965) Matrix formulation of electromagnetic scattering, *Proc. IEEE*, **53**: 805-812.

[17] Schenk, H.A. (1968) Improved integral formulation for acoustic radiation problems, J. *Acoust. Soc. Am.*, **44**: 41-58.

[18] Klein, C.A. and Mittra, R. (1975) An application of the "condition number" concept to the solution of scattering problems in the presence of the interior resonant frequencies, *IEEE Trans. Antennas and Propagat.*, **AP-23**: 431-435.

[19] Morita, N. (1979) Resonant solutions involved in the integral equation approach to scattering from conducting and dielectric cylinders, *IEEE Trans Antennas and Propagat.*, **AP-27**: 869-871.

[20] Roach, G.F. (1967) On the approximate solution of elliptic, self adjoint boundary value problems, *Arch. Ration. Mech. Anal.*, 27(3): 243-254; (1970) Approximate Green's functions and the solution of related integral equations, loc. cit., 36(1): 79-88.

[21] Ursell, F. (1973) On the exterior problems of acoustics, *Proc. Camb. Phil. Soc.*, **74**(1): 117-125.

[22] Jones, D.S. (1974) Integral equations for the exterior acoustic problem, *Q.J.* Mech. *Appl. Math.*, 27(1): 129-142.

[23] Brandt, D.W., Eftimiu, C., and Huddleston, P.L. (1985) Electromagnetic scattering by closed conducting bodies: the problem of internal resonances, *IEE Conference Publication 248*, 434-437, ICAP 1985.

If, however, the extended integral equations (1a) and (1b) are incorporated at points $\bar{r}$ on a surface S_δ parallel to, and a small distance $\delta > 0$ inside the current surface S of the perfect conductor (see Figure 1), by adding $\alpha\hat{n}$ cross Eqs. (1a) and (1b) at these points to the original MFIE Eq. (4a) and EFIE Eq. (4b), respectively, one obtains the "dual-surface" magnetic and electric-field integral equations:

$$\hat{n} \times \bar{H}_o(\bar{r}) = \frac{1}{2}\bar{K}(\bar{r}) - \hat{n} \times \oint_S \bar{K}(\bar{r}') \times \nabla'\psi_o(\bar{r},\bar{r}')dS' \qquad (5a)$$

($\bar{r}$ on S)

$$\hat{n} \times \bar{E}_o(\bar{r}) = \frac{\hat{n}}{i\omega\varepsilon_o} \times \oint_S \left[k^2 \bar{K}\psi_o - (\nabla'_s \cdot \bar{K})\nabla'\psi_o\right]dS', \qquad (5b)$$

where $\bar{E}_o$, $\bar{H}_o$ and ψ_o are defined as

$$\bar{E}_o(\bar{r}) \equiv \bar{E}_{inc}(\bar{r}) + \alpha\,\bar{E}_{inc}(\bar{r} - \delta\hat{n}) \qquad (6a)$$

$$\bar{H}_o(\bar{r}) \equiv \bar{H}_{inc}(\bar{r}) + \alpha\,\bar{H}_{inc}(\bar{r} - \delta\hat{n}) \qquad (6b)$$

$$\psi_o(\bar{r},\bar{r}') \equiv \psi(\bar{r},\bar{r}') + \alpha\,\psi(\bar{r} - \delta\hat{n},\ \bar{r}'). \qquad (6c)$$

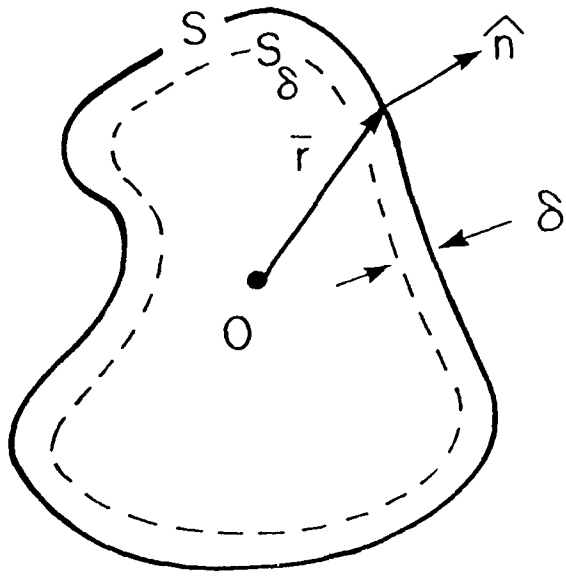

Figure 1. Geometry of a Perfect C luctor with Current Surface S and Parallel surface S_δ.

These dual-surface magnetic and electric-field integral equations, (5a) and (5b), although identical in form and comparable in complexity to the original MFIE (4a) and EFIE (4b), provide a unique solution for $\bar{K}$ at all real frequencies as long as the constant α is imaginary and the positive real constant δ is less than about $\lambda/2$. (In the numerical solutions of Eq. (5a) described in Section 4 below we choose α equal to i and δ equal to the smaller of about $\lambda/4$ or 1/4 the breadth of the scatterer along the normal at the point $\bar{r}$. Using α's of $\pm.5i$, $\pm i$, and $\pm 1.5i$. and varying δ from $\lambda/8$ to $3\lambda/8$ did not significantly change the computed solution, although the number of iterations required by the conjugate gradient method to attain the same value of normalized residual error varied somewhat with α and δ.)

3. UNIQUENESS OF SOLUTION OF THE DUAL-SURFACE INTEGRAL EQUATIONS

Uniqueness of solution for the dual-surface magnetic- and electric-field integral equations can be proven by considering the fields radiated by the solution currents. Concentrating on the dual-surface MFIE first, let $\bar{H}_s(\bar{r})$ be the magnetic field radiated by the solution $\bar{K}$ to Eq. (5a); specifically

$$\bar{H}_s(\bar{r}) = \int_S \bar{K}(\bar{r}) \times \nabla'\psi(\bar{r},\bar{r}')dS' \quad (\bar{r} \text{ not in } S). \tag{7}$$

If $\bar{K}$ were the correct unique current for this scattering problem, $\bar{H}_s(\bar{r})$ in Eq. (7) would be the correct scattered field for all $\bar{r}$ not in the surface current. However, since we do not know at this point that the solution $\bar{K}$ to Eq. (5a) is the correct unique solution, Eq. (7) simply defines an unknown magnetic field $\bar{H}_s(\bar{r})$.

Taking the curl of Eq. (7) twice reveals that this unknown magnetic field satisfies the homogeneous vector wave equation for all $\bar{r}$ not in the surface current $\bar{K}$, that is,

$$\nabla \times \nabla \times \bar{H}_s - k^2\bar{H}_s = 0 \qquad (\bar{r} \text{ not in } S). \tag{8}$$

Letting $\bar{r}$ approach S in Eq. (7) from the inside of S, and using the principal-value formula [Eq. (2)], we obtain

$$\bar{H}_s(\bar{r}\text{-}) = \frac{1}{2}\hat{n} \times \bar{K}(\bar{r}) + \oint_S \bar{K}(\bar{r}') \times \nabla'\psi(\bar{r},\bar{r}')\, dS' \qquad (\bar{r} \text{ on } S), \tag{9}$$

where $\bar{r}-$ in $\bar{H}_s(\bar{r}\text{-})$ indicates the field evaluated just inside the surface current. Since Eq. (7) holds for all $\bar{r}$ inside S, we can express $\bar{H}_s$ on the parallel surface S_δ as

$$\bar{H}_s(\bar{r} - \delta\hat{n}) = \oint_S \bar{K}(\bar{r}') \times \nabla' \psi(\bar{r} - \delta\hat{n}, \bar{r}') dS' \quad (\bar{r} \text{ on } S). \tag{10}$$

Add Eq. (9) to Eq. (10) multiplied by α and take $\hat{n}$ cross the result, to get

$$\hat{n} \times \left[(\bar{H}_s(\bar{r}-) + \alpha \bar{H}_s(\bar{r} - \delta\hat{n}) \right] = -\frac{1}{2} \bar{K}(\bar{r}) + \hat{n} \times \oint_S \bar{K}(\bar{r}') \times \nabla' \psi_o(\bar{r}, \bar{r}') dS'. \tag{11}$$
$$(\bar{r} \text{ on } S)$$

Comparing Eq. (11) with Eq. (5a), which $\bar{K}$ must also satisfy, reveals

$$\hat{n} \times \left[(\bar{H}_s(\bar{r}-) + \bar{H}_{inc}(\bar{r})) + \alpha \left(\bar{H}_s(\bar{r} - \delta\hat{n}) + \bar{H}_{inc}(\bar{r} - \delta\hat{n}) \right) \right] = 0 \quad (\bar{r} \text{ on } S). \tag{12}$$

The incident magnetic field also satisfies the vector wave equation

$$\nabla \times \nabla \times \bar{H}_{inc} - k^2 \bar{H}_{inc} = 0 \quad . \tag{13}$$

Thus, we can add Eq. (8) to Eq. (13), and rewrite Eq. (12) to arrive at the interior boundary value problem,

$$\nabla \times \nabla \times \bar{H} - k^2 \bar{H} = 0 \qquad (\bar{r} \text{ inside } S) \tag{14a}$$

$$\hat{n} \times \left[\bar{H}(\bar{r}) + \alpha \bar{H}(\bar{r} - \delta\hat{n}) \right] = 0 \qquad (\bar{r} \to S \text{ from inside}), \tag{14b}$$

where the total magnetic field $\bar{H}(\bar{r})$ is given by the sum of $\bar{H}_{inc}(\bar{r})$ and $\bar{H}_s(\bar{r})$.

The final steps of the uniqueness proof consist in showing that the boundary value problem defined by Eq. (14) has only the trivial solution, $\bar{H}(\bar{r}) = 0$, for the total field throughout the volume enclosed by the surface S, provided the constant α is imaginary

and the positive real constant δ is smaller than about $\lambda/2$. To show this, rewrite the boundary condition of Eq. (14b) explicitly for the magnetic field tangent to the surface S

$$H_t(\bar{r}) + \alpha\, H_t(\bar{r} - \delta\hat{n}) = 0 \quad (\bar{r}\rightarrow S \text{ from inside}). \tag{15}$$

The tangential magnetic fields, $H_t(\bar{r})$ and $H_t(\bar{r} - \delta\hat{n})$, are complex numbers that can be expressed in the form of a magnitude and phase

$$H_t(\bar{r}) = |H_t(\bar{r})|e^{i\phi(\bar{r})} \tag{16a}$$

$$(\bar{r}\rightarrow S \text{ from inside})$$

$$H_t(\bar{r} - \delta\hat{n}) = \left[|H_t(\bar{r})| + \Delta H_t(\bar{r},\delta)\right]e^{i\left[\phi(\bar{r}) + \Delta\phi(\bar{r},\delta)\right]} \tag{16b}$$

where ΔH_t and $\Delta\phi$ are the differences between the magnitudes and phases of $H_t(\bar{r})$ and $H_t(\bar{r} - \delta\hat{n})$. Insert $H_t(\bar{r})$ and $H_t(\bar{r} - \delta\hat{n})$ from Eq. (16) into Eq. (15) to get

$$|H_t| + \alpha\left(|H_t| + \Delta H_t\right)\left(\cos\Delta\phi + i\sin\Delta\phi\right) = 0. \tag{17}$$

Because $|H_t|$, ΔH_t, and $\Delta\phi$ are real numbers, if we let the constant α be an imaginary number($i\alpha_i$), the real and imaginary parts of Eq. (17) equate separately to give

$$|H_t| - \alpha_i\left(|H_t| + \Delta H_t\right)\sin\Delta\phi = 0 \tag{18a}$$

$$\alpha_i\left(|H_t| + \Delta H_t\right)\cos\Delta\phi = 0 \quad . \tag{18b}$$

For small δ, $\Delta\phi$ will be small - certainly not $\pm 90^{\circ}$* - and thus Eqs. (18) imply $|H_t| = 0$ and $\Delta H_t = 0$, or

$$H_t(\bar{r}) = 0 \qquad (r \to S \text{ from inside}) \tag{19a}$$

$$H_t(\bar{r} - \delta\hat{n}) = 0. \tag{19b}$$

In other words, when the constant α is chosen imaginary and δ is not large, the two separated tangential fields in the boundary condition of Eq. (14b) are each zero. That is, the tangential magnetic field on both the surface S and S_δ are zero.

The boundary condition of Eq. (19a) restricts the nonzero solutions of Eq. (14a) to the resonant modes of the cavity formed by a perfectly magnetically conducting surface S. These modes, which exist for a given cavity only at discrete frequencies, form standing waves within the cavity with magnetic and electric fields that can be chosen real and imaginary, respectively.[24] In particular, the tangential magnetic field near the surface S can be expressed approximately as

$$H_t(\bar{r}_s, r_n) \approx A(\bar{r}_s, r_n) \sin \gamma r_n \tag{20a}$$

where $(\bar{r}_s, r_n)$ are the coordinates tangent and normal to the surface S, γ is a positive real propagation constant with a value equal to or less than the propagation constant k of free space, and the amplitude $A(\bar{r}_s, r_n)$ varies with r_n slowly compared to the variation of $\sin \gamma r_n$. (With respect to the r_n direction the cavity can be considered a shorted waveguide with varying cross section.) If we let $r_n = 0$ on the surface S, the

---

*The one exception would be if there were a zero of H_t near the surface S or S_δ. In that case we can expand the boundary condition of Eq. 15 along the normal direction r_n in a Taylor series about the zero to show that $\partial H_t/\partial r_n$ must also vanish at the zero of H_t for imaginary α and small δ. Since Eq. (20a) shows that no cavity can support modes with both the tangential field and its normal derivative zero on its surface, the solution to Eq. (14) is unique in this exceptional case as well.

[24] Borgnis, F.E. and Papas, C.H. (1958) Electromagnetic waveguides and resonators, *Encyclopedia of Physics*, **16** Ed. S. Flugge, Springer-Verlag, Berlin.

boundary condition of Eq. (19a) is satisfied by (20a). The boundary condition of Eq. (19b) applied to (20a) requires that

$$\gamma\delta = m\pi \tag{20b}$$

for m equal to a positive integer. (We assume that there will be some portion of the surface S where A will not be zero. For if the tangential magnetic field were zero throughout the volume between S and S_δ, the fields would be zero throughout the cavity. Also, if degenerate modes exist, we assume their H_t fields will be linearly independent over the surface S_δ and thus Eq. (20b) will still hold. Because the maximum value of γ is $k = 2\pi/\lambda$, the condition of Eq. (20b) cannot be satisfied for

$$0 < \delta \lesssim \lambda/2 \ . \tag{21}$$

The approximate sign is included in the right side of the inequality in (21) because (20a) is an approximate expression for the standing wave field near the surface. If we look specifically at the resonant cavity formed by shorting the ends of a waveguide of arbitrary uniform cross section, we find (20a) applies exactly with A equal to a constant. Thus, the inequality of (21) holds exactly for a shorted waveguide cavity. For a spherical cavity the fields vary radially as spherical Bessel functions of the first kind. For asymptotically large spheres, (20a) again holds exactly, and for all spheres large enough to sustain resonant modes, (20a) holds to a good approximation near the surface - thereby confirming the approximate inequality [Eq. (21)] for spherical cavities.

In summary, the only solution to Eq. (14) for α imaginary and $0 < \delta \lesssim \lambda/2$ is the trivial solution, $\bar{H}(\bar{r}) = \bar{H}_{inc}(\bar{r}) + \bar{H}_s(\bar{r}) = 0$ throughout the volume enclosed by S. Since $\bar{E} = -\nabla \times \bar{H}/i\omega\varepsilon_o$, the electric field $\bar{E}(\bar{r}) = \bar{E}_{inc}(\bar{r}) + \bar{E}_s(\bar{r})$ within this volume is also identically zero. And, as mentioned in Section 2, it is a simple matter to prove[16] that the current that produces the negative of the incident electromagnetic fields throughout the volume enclosed by S is the correct unique current for the exterior scattering problem. (Namely, $\bar{E}$ and $\bar{H}$ equaling zero inside S implies $\hat{n} \times \bar{E} = 0$ and $\hat{n} \times \bar{H} = \bar{K}$ for the fields just outside S -- the conditions required for uniqueness of solution of the

exterior problem[25].) Since this unique solution has been derived from the solution current of Eq. (5a), the dual-surface magnetic-field integral equation (5a) has a unique solution.

Beginning with the solution current of the dual-surface electric-field integral equation (5b), and defining the electric field

$$E_s(\bar{r}) = -\frac{1}{i\omega\varepsilon_0}\int_S \left[k^2 K\psi - (\nabla'_s \cdot K)\nabla'\psi\right] dS' \quad (r \text{ not in } S) \tag{22}$$

initially, instead of the magnetic field Eq. (7), we obtained the same inequality (21) as the sufficient condition for the uniqueness of solution of the dual-surface electric-field integral equation (5b).

In numerical practice, we suggest choosing α equal to i to weight the fields on S and S_δ equally in the boundary condition [Eq. (14b)] by an imaginary constant. Likewise, we suggest choosing δ equal to about $\lambda/4$, to keep the surface S_δ about an equal distance between the two critical values, $\delta = 0$ and $\lambda/2$. The dual-surface integral equations allow spurious solutions at $\delta = 0$ where they reduce to the original integral equations (4), and at δ equal to or greater than about $\lambda/2$ where the dual-surface boundary condition [Eq. (14b)] no longer insures uniqueness of solution. When the breadth of the scatterer along the normal is less than λ, one can choose δ equal to 1/4 the breadth instead of $\lambda/4$.

A numerical demonstration of the elimination of the spurious resonances by the dual-surface magnetic-field integral equation is given in Figures 2 and 3. Figure 2 plots the total (integrated) radar cross section versus the perimeter of a perfectly conducting cube of side length s as computed using the conventional magnetic field integral equation (4a). The spurious resonances begin to contaminate the MFIE solution in Figure 2 near the first resonance of the cube at $4s/\lambda = 2.8$ and continue to distort the solution at an increasing rate commensurate with the increasing density of resonant frequencies. Figure 3 shows clearly that the dual-surface magnetic-field integral equation (5a) eliminates the spurious resonances from the MFIE solution in Figure 2.

[25] Muller, C. (1969) *Foundations of the Mathematical Theory of Electromagnetic Waves*, Springer-Verlag, New York, Theorem 71.

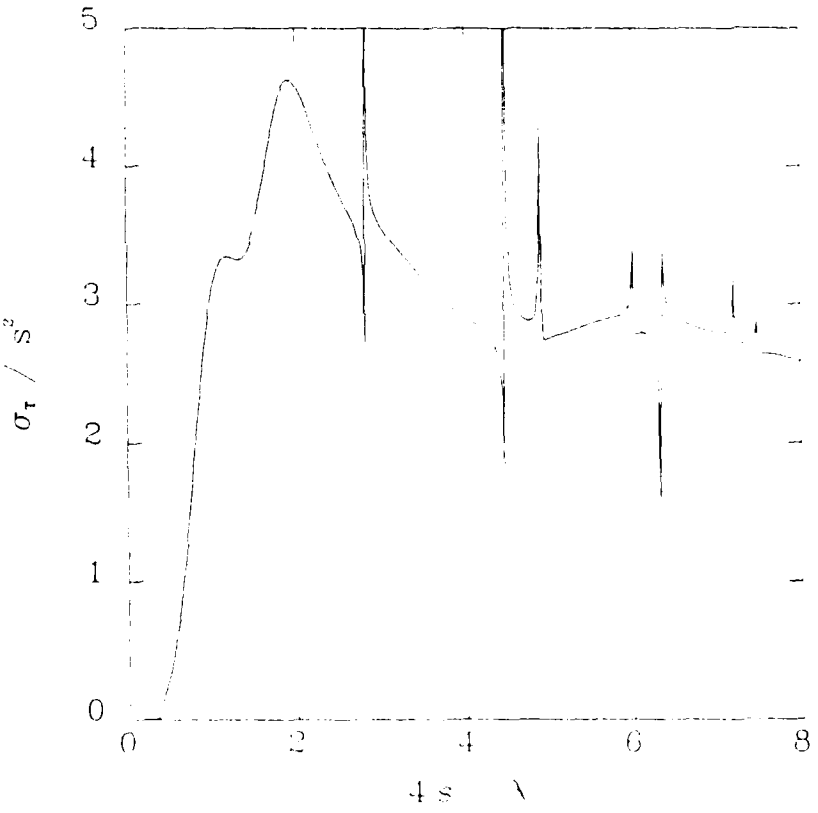

Figure 2. Total Radar Cross Section Versus Perimeter of a Perfectly Conducting Cube as Computed with the Conventional Magnetic-Field Integral Equation (4a).

Figure 3. Total Radar Cross Section Versus Perimeter of a Perfectly Conducting Cube as Computed with the Dual-Surface Magnetic-Field Integral Equation (5a).

4. NUMERICAL SOLUTION TO THE DUAL-SURFACE MAGNETIC-FIELD INTEGRAL EQUATION BY THE CONJUGATE GRADIENT METHOD

The similarity of the dual-surface integral equations (5) to the original integral equations (4) allows them to be solved numerically by a minor modification to existing MFIE and EFIE computer programs. One merely adds the values of the incident field and free-space Green's function (each multiplied by α) at the points $\bar{r} - \delta\hat{n}$ to their respective values at $\bar{r}$ used in the computer programs of the original integral equations. In particular, we consider a straightforward numerical solution to the dual-surface magnetic-field integral equation (5a) for scattering from the perfect conductor S.

Divide the surface S of the scatterer into M patches, assume the current is a constant vector over each patch, approximate the value of the Green's function $\nabla'\psi_o$ over each patch by a constant vector equal to the value of $\nabla'\psi_o$ at the center of the patch, and apply the integral equation (5a) at the center of each patch. In short, approximate the integral in Eq. (5a) by the summation

$$\hat{n}_i \times \bar{H}_o(\bar{r}_i) = \frac{1}{2}\bar{K}(\bar{r}_i) - \hat{n}_i \times \sum_{\substack{j=1 \\ (j\neq i)}}^{M} \bar{K}(\bar{r}_j) \times \nabla'\psi_o(\bar{r}_i, \bar{r}_j)\Delta S_j \qquad i = 1,2,\ldots..M \tag{23}$$

where ΔS_j is the area of each patch, and the self-patch (i = j) in the summation is taken as the "principal area"[8] excluded by the principal-value integral in Eq. (5a). (In the language of the method of moments, we have used pulse basis functions and delta testing functions.)

For each patch there are two complex unknown components of surface current $\bar{K}$ and two complex scalar equations. Thus, Eq. (23) represents a simultaneous set of 2M linear complex equations for 2M complex unknowns, and can be written in tensor notation as

$$a_{ij}\, x_j = b_i, \quad i = 1,2, \ldots.N = 2M, \tag{24}$$

where the x_j are the complex unknown components of surface current, the a_{ij} are the elements of the given coefficient matrix, and the b_i are the given incident-field values. Summation from 1 to N over the repeated index j in Eq. (24) is, of course, implied.

In solving Eq. (24) for three-dimensional bodies on readily available computers, one quickly encounters the problem of limited central or virtual memory and excessive computer time as the size of the body is increased beyond a wavelength. For example, we have found that the dual-surface MFIE requires a minimum of about 25 patches per square wavelength* to achieve reasonable accuracy in the computed currents and far fields. A cube of side length s thus requires about $M = 150\ (s/\lambda)^2$ patches or

$$N = 2M = 300(s/\lambda)^2 \tag{25}$$

complex unknowns, and a memory of

$$W = 2N^2 \tag{26}$$

real words W to store the complex $N \times N$ matrix with elements a_{ij}. On our VAX 8650 with an allotted virtual memory of one million words, the solution of Eq. (24) is limited to cubes less than about 1.5 wavelengths on a side. (Paging time became excessive as the amount of virtual memory used approached a million words; and allotting more virtual memory to the computer was not as efficient an alternative as using direct access files for increasing computer storage capacity.[26]) Moreover, we found that

---

* This requirement of about 5 linear divisions per wavelength to get reasonable accuracy is not surprising if one considers that the current and the Green's function in the surface integral equation varies along the surface of the scatterer with a maximum spatial frequency equal to about one cycle per wavelength. This means that the product of the current and Green's function in the integral of the integral equation has a maximum spatial frequency of about 2 cycles per wavelength. The sampling theorem would then require about 4 samples per linear wavelength to accurately approximate the integral of the current times the Green's function by a summation.

[26] Perry, T.S. and Zorpette, G. (1989) Supercomputer experts predict expansive growth, *IEEE Spectrum*, **26**: 26-33.

solving Eq. (24) using Gaussian elimination on this computer with a 32-bit Linpack performance rating[5] of 1.3 megaflops took a CPU time T_{GE} given approximately (for large N) by

$$T_{GE} = 2.2 \times 10^{-7} N^3 \tag{27}$$

minutes, which becomes prohibitive for cubes greater than about 2 wavelengths on a side. Incorporating two-fold symmetry of the cube to reduce N by a factor of 4 still did not allow us, in a reasonable computer time, to solve for scattering from cubes larger than about 4 wavelengths on a side using Gaussian elimination on the available computer. The fastest available computers (those with 32-bit Linpack performance ratings of about 100 megaflops) would take many hours of computer time to solve Eq. (24) using Gaussian elimination for general 3-D scatterers larger than a few wavelengths across. Even with massive vector parallelism it is difficult to conceive of digital computers extending appreciably the formidable restriction on s/λ presented by the $(s/\lambda)^6$ dependence of the computer time in Eq. (27) for solving Eq. (24) using Gaussian elimination.

To extend the limits of computer storage and processing time on the available mainframe, we made use of direct access memory files on disk and solved Eq. (24) iteratively using the conjugate gradient method rather than Gaussian elimination.[3] A direct access file was used to store the rows of the N × N complex matrix. The file could be either opened, written to, or read from by a single Fortran command, and increased our available memory from 1 million to 30 million words. (Of course, with iterative solvers one can greatly reduce computer storage requirements by generating the coefficient matrix during each iteration. However, this greatly increases the required CPU time.)

The drawbacks of using direct access files are the necessary additional computer programming, the somewhat greater CPU time, and possibly a large increase in input/output time. Use of direct access files roughly doubles the CPU time required to solve Eq. (24) using the conjugate gradient method. Gaussian elimination CPU times are either roughly doubled or multiplied by a factor of about 10, when using direct access files, depending on whether or not a round-off error check is included in the Gaussian elimination algorithm. (We shall discuss this later in conjunction with Tables 1 and 2.) The extra input/output time associated with the direct access files may dominate computer turn-around time on our computer system when the matrix is solved using the conjugate gradient method. Meaningful input/output times are elusive,

however, on central computers since they depend so strongly on the particular direct access system, the way the system is tuned, and the number of users sharing the machine.

We found the conjugate gradient iterative method an efficient alternative to Gaussian elimination for solving the large system of equations (24) generated by the dual-surface magnetic-field integral equation (5a) applied to 3-D multi-wavelength bodies. It converges in a finite number of steps for any initial guess, as long as the matrix is not singular and round-off errors are kept negligible. The flexibility of accepting any initial guess permits the user to stop the iteration and start using the current estimate for the solution as the new initial guess. This restarting eliminates the accumulated round-off errors, but requires an extra matrix multiplication, slows convergence, and increases the run time. Thus, restarting should be done only when necessary to reduce the round-off errors. For solving the dual-surface equations (23-24) on our 32-bit computer, it was sufficient to restart only once before the final step, even when N was as large as 3468. (Wang and Dubberley[27] discuss this restart problem.)

We used a version of the conjugate gradient method referred to as "Case A" in Reference 2. We applied the conjugate gradient algorithm to the matrix with elements a_{ij} in Eq. (24) rather than directly to the operator of the dual-surface magnetic-field integral equation (5a). Some justification for this may be found in the recent papers[28,29] where it is concluded that iterative techniques applied directly to the operator and implemented numerically contain an implicit discretization and, in many cases, a corresponding moment method interpretation. It is interesting that, as early as 1943, Hotelling[30] in his review of some new methods in matrix calculation commented that, "The combination of this device [Mallock electrical calculating machine] with the iterative method...

[27] Wang, J.J.H. and Dubberley, J.R. (1989) Computation of electromagnetic fields in large biological bodies by an iterative moment method with a restart technique, *IEEE Trans. Microwave Theory and Techniques*, MTT-37: 1918-1923.

[28] Ray, S.L. and Peterson, A.F. (1988) Error and convergence in numerical implementations of the conjugate gradient method, *IEEE Trans. Antennas Propagat.* **36**: 1824-1827.

[29] Sarkar, T.K., Yang, X., and Arvas, E. (1988) A limited survey of various conjugate gradient methods for solving complex matrix equations arising in electromagnetic wave interactions, *Wave Motion* **10**(6): 527-546.

[30] Hotelling, H. (1943) Some new methods in matrix calculation, *Annals of Math. Stat.*, **14**(1): 1-34.

offers what seems at present [1943] the best hope for the systematic inversion [solution] of large matrices."

Table 1 compares the number of major complex operations required to solve large matrices by means of Gaussian elimination and the conjugate gradient method, when using direct access memory files. Table 2 shows the associated CPU times required by our 32-bit, 1.3 megaflop Linpack-performance-rated VAX 8650 computer.

Table 1. Number of Complex Operations Required for N × N Matrix Solution Using Gaussian Elimination and the Conjugate Gradient Method.

METHOD	NUMBER OF OPERATIONS						
	Multiply	Add	Subtract	Do Loops	Elements Written	Elements Read	If
Gaussian Elim. (total)	$\frac{2}{3}N^3$	0	$\frac{1}{3}N^3$	$\frac{1}{3}N^3$	$\frac{1}{2}N^3$	$\frac{3}{2}N^3$	$\frac{1}{3}N^3$
Conjugate Grad. (per iteration)	$2N^2$	$2N^2$	0	$2N^2$	0	$2N^2$	0

Table 2. CPU Time Required for Complex Operations on Our 32-Bit, 1.3 Megaflop Linpack-Performance-Rated Computer.

OPERATION	CPU Time (10^{-6} sec)
Complex Add	0.84
Complex Subtract	0.96
Complex Multiply	2.03
Complex Divide	13.09
If	15.09
Do Loop	0.67
Read per complex element (for large N)	2.30
Write per complex element (for large N)	2.41

The CPU times for the complex operations in Table 2 can be inserted into Table 1 to estimate the total CPU times, t_{GE} and t_{CG}, for this computer to solve Eq. 24 by Gaussian elimination and the conjugate gradient method. Specifically,

$$t_{GE} = 1.93 \times 10^{-7} N^3 \tag{28}$$

$$t_{CG} = 1.95 \times 10^{-7} N^2 I \tag{29}$$

minutes, where N is, as usual, the dimension of the complex matrix, and I is the number of iterations needed for convergence using the conjugate gradient method. Comparing the estimated CPU time [Eq. (28)], for the solution to scattering from the cube by Gaussian elimination, with the actual CPU run times (for the whole program) given approximately by the formula (27), one finds that the estimated time [Eq. (28)] is about 90 percent of the actual total CPU run times. Likewise, Eq. (29) gives an estimated CPU time for the conjugate gradient method that is about 75 percent of the actual total CPU times for scattering from large cubes (see Table 3). The additional 10 percent and 25 percent CPU times are taken mainly by matrix-fill, complex conjugate, and miscellaneous overhead operations.

Table 3. Number of Iterations (I) and Actual Total CPU Time Using the Conjugate Gradient Method on our 32-Bit, 1.3 Megaflop Linpack-Performance-Rated Computer.

s/λ	N	Patches/λ^2	I	I/N	CPU Time (h:m:s)
0.75	48	28	35	.73	0:00:04
0.75	108	63	39	.36	0:00:12
0.75	192	112	42	.22	0:00:32
1.5	192	28	61	.32	0:00:45
1.5	432	63	62	.14	0:03:08
1.5	768	113	61	.08	0:10:47
2.4	432	25	83	.19	0:04:29
2.4	768	44	82	.11	0:13:53
2.4	1200	69	88	.07	0:35:15
3.0	768	28	90	.12	0:13:30
3.0	1200	44	92	.08	0:33:21
3.0	1728	63	93	.05	1:09:44
5.0	1728	23	118	.07	1:25:47
5.0	3468	46	119	.03	6:23:10
6.75	3468	25	141	.04	7:28:34

The time estimates Eqs. (28) and (29) reveal that, for our typical computer, the solution to Eq. (24) by the conjugate gradient method will take less computer time than Gaussian elimination if the number of required iterations I is less than N. This conclusion holds whether or not direct access files are used, because including the write and read statements from Table 1 due to the use of direct access files roughly doubles, as mentioned above, the computer times for both Gaussian elimination (with round-off error check) and the conjugate gradient method.

It is important to note, however, that the logical IF operations and one half the multiplication operations listed in Table 1 for Gaussian elimination are produced by the round-off error check in our Gaussian elimination algorithm. If this round-off error check is omitted, the revised Gaussian elimination CPU time t'_{GE} estimated from Tables 1 and 2 is given by

$$t'_{GE} = 10^{-7}\ N^3 \tag{30}$$

minutes, about one half the CPU times given by Eq. (27) or (28). Comparing Eq. (30) with Eq. (29) shows that the conjugate gradient method becomes faster than Gaussian elimination without the round-off error check when the number of iterations I is less than about N/2.

If in addition to omitting the round-off error check from the Gaussian elimination algorithm, all computations could be done in central memory without using direct access files, the write and read operations would be eliminated from Table 1, and CPU times [Eqs. (28) and (29)], would be replaced by

$$t^{O}_{GE} = 0.2 \times 10^{-7}\ N^3 \tag{31}$$

$$t^{O}_{CG} = 1.2 \times 10^{-7}\ N^2 I \tag{32}$$

minutes. Comparison of Eqs. (31) and (32) reveals that, if all computations can be handled in central memory, the conjugate gradient method is faster than Gaussian

elimination (without a round-off error check) when the number of required iterations is less than about N/6.[31]

Table 3 lists the number of iterations and actual CPU times using the conjugate gradient method for the dual-surface magnetic-field equations, (23-24), applied to plane-wave scattering from a perfectly conducting cube.[4] The plane wave was incident broadside upon the cube of side length s, and the parameters α and δ in the dual-surface magnetic-field integral equation (5a) were set equal to 1 and $3/16\ \lambda$, respectively. The initial value taken for the solution vector in the conjugate gradient algorithm was zero, and the iterations were terminated when the ratio of the magnitude of the residual vector to the magnitude of the source vector became less than 10^{-6}. Two-fold (xy) symmetry of the cube was used to reduce the number of unknowns N in Table 3 by a factor of 4, so that N equals $75(s/\lambda)^2$ rather than $300(s/\lambda)^2$ [see Eq. (25)] for N in terms of the side-to-wavelength ratio (s/λ) of a cube with 25 patches per square wavelength, the minimum number needed to achieve reasonable accuracy in the computed surface currents and far fields.

Table 3 reveals that the number of required iterations depends mainly on the side-to-wavelength ratio of the cube, and hardly at all on the number of patches per square wavelength or, equivalently, hardly at all on the number of unknowns N for a fixed s/λ (assuming a reasonable minimum number of patches per square wavelength are used). This independence of the number of conjugate gradient iterations on the cell density has also been observed in the solution to two-dimensional scattering problems.[32,33] Since the CPU time is proportional to the total number of patches, the CPU time for the conjugate gradient solution is minimized by choosing the least number of patches per square wavelength sufficient for the desired solution accuracy (approximately 25 patches per square wavelength in our case).

The number of iterations I_{25} required for convergence with the conjugate gradient method as a function of the number of unknowns N, when using the minimum patch density

---

[31] Wheeler III, J.E. and Wilton, D.R. (1988) Comparison of convergence rates of the conjugate gradient method applied to various integral equation formulations, *Digest of the IEEE AP-S Symposium*, Syracuse, NY, pp. 229-232.

[32] Peterson, A.F. and Mittra, R. (1986) Convergence of the conjugate gradient method when applied to matrix equations representing electromagnetic scattering problems, *IEEE Trans. Antennas Propagat.* **AP-34**: 1447-1454.

[33] Peterson, A.F., Smith, C.F., and Mittra, R. (1988) Eigenvalues of the moment-method matrix and their effect on the convergence of the conjugate gradient alrorithm, *IEEE Trans. Antennas Propagat.* **36**:1177-1179.

of about 25 per square wavelength [$N \approx 75(s/\lambda)^2$], appears from Table 3 to approach a logarithmic function of N as N gets large; specifically

$$I_{25} \approx 33 \ln(.02N) = 66 \ln(1.25\ s/\lambda). \tag{33}$$

Substituting I_{25} for I in Eq. (29) [divided by .75 since Eq. (29) gives a predicted value that is about 75 percent of the actual CPU run time] gives

$$T_{CG} \approx 8.5 \times 10^{-6}\ N^2 \ln(.02N) \approx .1(s/\lambda)^4 \ln(s/\lambda) \tag{34}$$

minutes, as an estimate of the CPU time required to solve for scattering from large cubes by the conjugate gradient method on our 32-bit, 1.3 megaflop Linpack-performance-rated computer. (Interestingly, Catedra et al.[34] also found a CPU time dependence proportional to the right side of Eq. (34) when solving 3-D scattering problems using the conjugate gradient fast Fourier transform method applied to a volume electric-field integral equation.) Because the logarithmic function is so slowly varying, Eq. (34) implies that the CPU time for solving full-bodied, 3-D, multi-wavelength scatterers with well-behaved surface integral equations increases roughly as the fourth power of the electrical size of the scatterer.

In Figure 4 the conjugate gradient and Gaussian elimination CPU times vs s/λ for scattering from the cube are plotted from Eqs. (34) and (30) [with $N = 75(s/\lambda)^2$] by the solid and dashed lines, respectively. Even though two-fold symmetry of the cube has been utilized to reduce the number of unknowns N by the factor of 4, Figure 4 confirms that Gaussian elimination CPU time becomes prohibitive for cubes larger than a few wavelengths across, and that conjugate gradient iteration allows one to determine scattering from considerably larger bodies.

---

[34] Catedra, M.F., Gago, E., and Nuno, L. (1989) A numerical scheme to obtain the RCS of three-dimensional bodies of resonant size using the conjugate gradient method and the fast Fourier transform, *IEEE Trans. Antennas and Propagat.*, 37: 528-537.

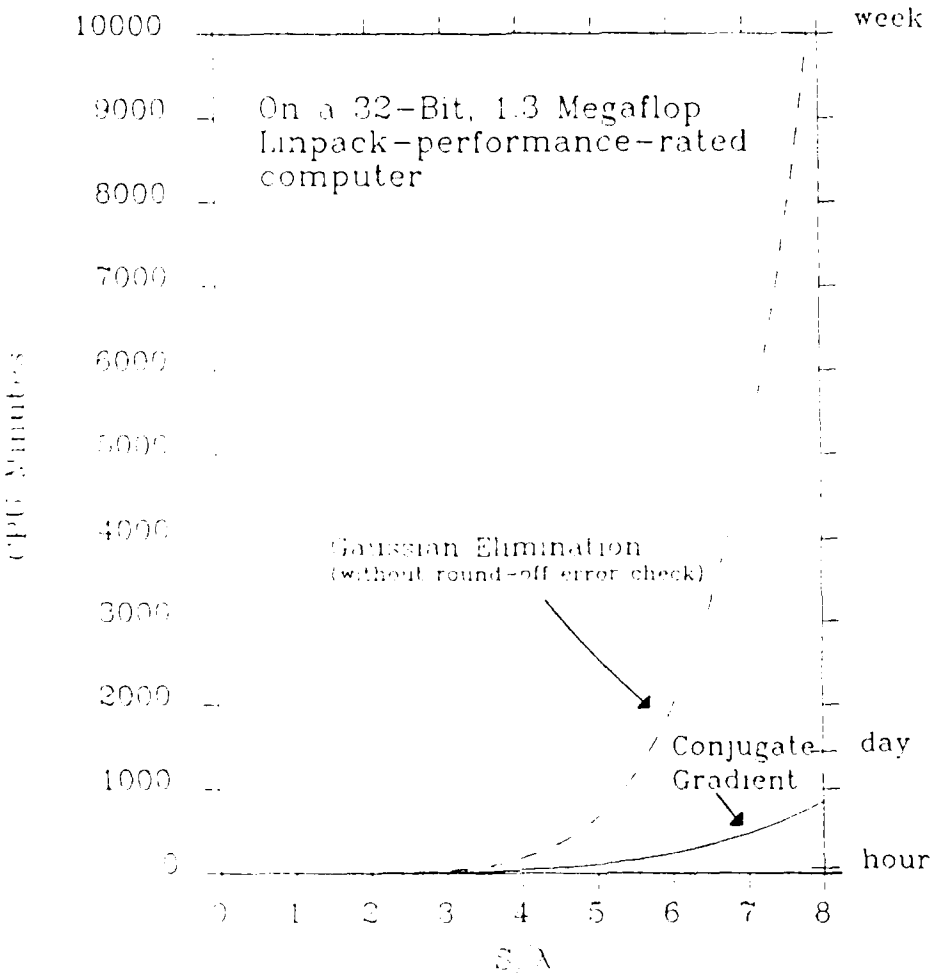

Figure 4. CPU Time Versus Side-Length to Wavelength Ratio for Dual-Surface Magnetic-Field Integral Equation Solution for Scattering from a Perfectly Conducting Cube. The number of unknowns N is given by 75 $(s/\lambda)^2$, since two-fold symmetry of the cube was used to reduce the number of unknowns by a factor of four and the fixed patch density is 25 per square wavelength. The conjugate gradient and Gaussian elimination times shown here would be reduced by factors of about two and five, respectively, if the coefficient matrices could be stored in central memory rather than in direct access files, that is, if the CPU time were computed from Eqs. (32) and (31) instead of Eqs. (34) and (30).

We emphasize that the formula (34) for the conjugate gradient CPU time as a function of the number of unknowns and electrical size of the scatterer is an approximation obtained by solving for scattering from the perfectly conducting cube using the magnetic-field dual-surface integral equation. The formula holds for a patch density of about 25 patches per square wavelength and a normalized residual of 10^{-6}. Since the number of iterations is nearly independent of patch density, higher patch densities will increase the CPU time proportionately. The CPU time will decrease if the normalized residual is chosen greater than 10^{-6}; in particular, we found that the number of iterations and thus CPU time halved when the normalized residual was increased from 10^{-6} to a value between 10^{-3} and 10^{-2}. As mentioned in Section 2, the number of iterations and CPU time will also vary somewhat with the chosen values of the parameters α and δ in the dual-surface integral equation, but this variation was not large for values of α between ± 1.5 i and δ between $\lambda/8$ and $3\lambda/8$.

We also applied the magnetic-field dual-surface integral equation to rectangular boxes with side-length ratios that differed considerably from the value of unity for the cube. For some rectangular boxes, the required number of iterations and CPU time were appreciably larger than the values predicted by Eqs. (33) and (34) for a cube of the same surface area, but T_{CG} in Eq. (34) was never larger than $8.5 \times 10^{-6}\ N^{5/2}$. Although the incident plane wave always propagated normally to the xy face of the rectangular boxes (broadside incidence), it is unlikely that the N-dependence of T_{CG} in Eq. (34) would change dramatically with the direction of the incident plane wave, because the formulation took advantage of the xy symmetry that results from the broadside incidence to reduce the number of unknowns N in the coefficient matrix by a factor of 4.

Finally, in hopes of reducing computer time further, we experimented with three variations of the conventional conjugate gradient method, namely the "biconjugate" gradient method, the "augmented" conjugate gradient method, and the "modified" conjugate gradient method.[29,35] We found that for the three dimensional, multi-wavelength problem solved with surface integral equations, these three variations converged more slowly than the conventional conjugate gradient method, regardless of the initial guess, or whether they were used alone or in conjunction with the conventional conjugate gradient method.[3]

---

[35] Sarkar, T.K. (1987) On the application of the generalized biconjugate gradient method, *J. Electromagnetic Waves and Applications*, 1(3): 223-242.

REFERENCES

1 Tobin, A.R., Yaghjian, A.D., and Bell, M.M. (1987) Surface integral equations for multi-wavelength, arbitrarily shaped, perfectly conducting bodies, *Digest of the National Radio Science Meeting (URSI)*, Boulder, CO, p.9.

2 Sarkar, T.K., and Arvas, E. (1985) On a class of finite step iterative methods (conjugate directions) for the solution of an operator equation arising in electromagnetics, *IEEE Trans. Antennas and Propagation*, **AP-33**, 1058-1066.

3 Woodworth, M.B. (1988) *Large Matrix Solution Techniques Applied to an Electromagnetic Scattering Problem.* RADC-TR-88-268. ADA206917

4 Cote, M.G., Woodworth, M.B., and Yaghjian, A.D. (1988) Scattering from the perfectly conducting cube, *IEEE Trans. Antennas Propagat.*, **AP-36**: 1321-1329.

5 Dongarra, J., Martin, J.L., and Worlton, J. (1987) Computer benchmarking: paths and pitfalls, *IEEE Spectrum*, **24**: 38-43.

6 Murray, F.H. (1931) Conductors in an electromagnetic field, *Am. J. Math.*, **53**: 275-288.

7 Maue, A.W. (1949) On the formulation of a general scattering problem by means of an integral equation, *Z. Phys.*, **126**(7/9): 601-618.

8 Yaghjian, A.D. (1981) Augmented electric and magnetic-field integral equations, *Radio Science*, **16**: 987-1001.

9 Mitzner, K.M. (1968) Numerical solution of the exterior scattering problem at eigen-frequncies of the interior problem, *Digest of Fall URSI Meeting*, Boston, MA, p. 75.

10 Poggio, A.J., and Miller, E.K. (1973) Integral equation solutions of three-dimensional scattering problems, in *Computer Techniques for Electromagnetics*, edited by R. Mittra, pp. 159-264, Pergamon, New York.

11 Mautz, J.R., and Harrington, R.F. (1978) H-field, E-field, and combined-field solutions for conducting bodies of revolution, *Arch. Elecktron. Ubertragungstech. (Electron. Commun.)*, 32(4): 157-164.

12 Panic, I.O. (1965) On the solvability of exterior boundary-value problems for the wave equation and for a system of Maxwell's equations, *Uspehi Mat. Nauk*, 20(1): 221-226.

13 Brakhage, H., and Werner, P. (1965) Uber das Dirichletsche Aussenraumproblem fur die Helmholtzsche Schwingungsgleichung, *Arch. Math.*, 16, 325-329.

14 Mautz, J.R., and Harrington, R.F. (1979) A combined-source solution for radiation and scattering from a perfectly conducting body, *IEEE Trans. Antennas and Propagat.*, AP-27: 445-454.

15 Toyoda, I., Matsuhara, M., and Kumagai, N. (1988) Extended integral equation formulation for scattering problems from a cylindrical scatterer, *IEEE Trans. Antennas and Propagat.*, 36: 1580-1586.

16 Waterman, P.C. (1965) Matrix formulation of electromagnetic scattering, Proc. *IEEE*, 53: 805-812.

17 Schenk, H.A. (1968) Improved integral formulation for acoustic radiation problems, *J. Acoust. Soc. Am.*, 44: 41-58.

18 Klein, C.A., and Mittra, R. (1975) An application of the "condition number" concept to the solution of scattering problems in the presence of the interior resonant frequencies, *IEEE Trans. Antennas and Propagat.*, AP-23: 431-435.

19 Morita, N. (1979) Resonant solutions involved in the integral equation approach to scattering from conducting and dielectric cylinders, *IEEE Trans. Antennas and Propagat.*, AP-27: 869-871.

20 Roach, G.F. (1967) On the approximate solution of elliptic, self adjoint boundary value problems, *Arch. Ration. Mech. Anal.*, 27(3): 243-254; (1970) Approximate Green's functions and the solution of related integral equations, loc.cit., 36(1): 79-88.

21 Ursell, F. (1973) On the exterior problems of acoustics, *Proc. Camb. Phil. Soc.*, 74(1): 117-125.

22 Jones, D.S. (1974) Integral equations for the exterior acoustic problem, *Q.J. Mech. Appl. Math.*, 27(1): 129-142.

23 Brandt, D.W., Eftimiu, C., and Huddleston, P.L. (1985) Electromagnetic scattering by closed conducting bodies: the problem of internal resonances, *IEE Conference Publication 248*, 434-437, ICAP 1985.

24 Borgnis, F.E., and Papas, C.H. (1958) Electromagnetic waveguides and resonators, *Encyclopedia of Physics*, **16**, Ed. S. Flugge, Springer-Verlag, Berlin.

25 Muller, C. (1969) *Foundations of the Mathematical Theory of Electromagnetic Waves*, Springer-Verlag, New York, Theorem 71.

26 Perry, T.S., and Zorpette, G. (1989) Supercomputer experts predict expansive growth, *IEEE Spectrum*, **26**: 26-33.

27 Wang, J.J.H., and Dubberley, J.R. (1989) Computation of electromagnetic fields in large biological bodies by an iterative moment method with a restart technique, *IEEE Trans. Microwave Theory and Techniques*, **37**, 1918-1923.

28 Ray, S.L., and Peterson, A.F. (1988) Error and convergence in numerical implementations of the conjugate gradient method, *IEEE Trans. Antennas and Propagat.*, **36**: 1824-1827.

29 Sarkar, T.K., Yang, X., and Arvas, E. (1988) A limited survey of various conjugate gradient methods for solving complex matrix equations arising in electromagnetic wave interactions, *Wave Motion*, **10**(6): 527-546.

30 Hotelling, H. (1943) Some new methods in matrix calculation, *Annals of Math. Stat.*, **14**(1): 1-34.

31 Wheeler III, J.E. and [illegible]ton, D.R. (1988) Comparison of convergence rates of the conjugate gradient method applied to various integral equation formulations, *Digest of the IEEE AP-S Symposium*, Syracuse, NY, pp. 229-232.

32 Peterson, A.F., and Mittra, R. (1986) Convergence of the conjugate gradient method when applied to matrix equations representing electromagnetic scattering problems, *IEEE Trans. Antennas and Propagat.*, **AP-34**: 1447-1454.

33 Peterson, A.F., Smith, C.F., and Mittra, R. (1988) Eigenvalues of the moment-method matrix and their effect on the convergence of the conjugate gradient algorithm, *IEEE Trans. Antennas and Propagat.*, **36**: 1177-1179.

34 Catedra, M.F., Gago, E., and Nuno, L. (1989) A numerical scheme to obtain the RCS of three-dimensional bodies of resonant size using the conjugate gradient method and the fast Fourier transform, *IEEE Trans. Antennas and Propagat.*, **37**: 528-537.

35 Sarkar, T.K. (1987) On the application of the generalized biconjugate gradient method, *J. Electromagnetic Waves and Applications*, **1**(3): 223-242.

MISSION
of
Rome Air Development Center

RADC plans and executes research, development, test and selected acquisition programs in support of Command, Control, Communications and Intelligence (C^3I) activities. Technical and engineering support within areas of competence is provided to ESD Program Offices (POs) and other ESD elements to perform effective acquisition of C^3I systems. The areas of technical competence include communications, command and control, battle management, information processing, surveillance sensors, intelligence data collection and handling, solid state sciences, electromagnetics, and propagation, and electronic, maintainability, and compatibility.